Traffic
doi:10.1111/tra.12350

Human Peroxin PEX3 Is Co-translationally Integrated into the ER and Exits the ER in Budding Vesicles

Peter U. Mayerhofer[1,2,3,*], Manuel Bañó-Polo[4], Ismael Mingarro[4] and Arthur E. Johnson[1,5,6,*]

[1]Department of Molecular and Cellular Medicine, Texas A&M Health Science Center, 440 Reynolds Medical Building, College Station, TX 77843, USA
[2]Institute of Biochemistry, Biocenter, Goethe University Frankfurt, Max-von-Laue Str. 9, 60438 Frankfurt, Germany
[3]Present address: School of Biosciences & Medicine, University of Surrey, Guildford GU2 7XH, UK
[4]Departament de Bioquimica i Biologia Molecular, Universitat de Valencia, C/ Dr. Moliner, 50, E-46100 Burjassot, Spain
[5]Department of Chemistry, Texas A&M University, College Station, TX 77843, USA
[6]Department of Biochemistry and Biophysics, Texas A&M University, College Station, TX 77843, USA
*Corresponding authors: Peter U. Mayerhofer, mayerhofer@em.uni-frankfurt.de, p.mayerhofer@surrey.ac.uk and Arthur E. Johnson, ajohnson@medicine.tamhsc.edu

Abstract

The long-standing paradigm that all peroxisomal proteins are imported post-translationally into pre-existing peroxisomes has been challenged by the detection of peroxisomal membrane proteins (PMPs) inside the endoplasmic reticulum (ER). In mammals, the mechanisms of ER entry and exit of PMPs are completely unknown. We show that the human PMP PEX3 inserts co-translationally into the mammalian ER via the Sec61 translocon. Photocrosslinking and fluorescence spectroscopy studies demonstrate that the N-terminal transmembrane segment (TMS) of ribosome-bound PEX3 is recognized by the signal recognition particle (SRP). Binding to SRP is a prerequisite for targeting of the PEX3-containing ribosome•nascent chain complex (RNC) to the translocon, where an ordered multistep pathway integrates the nascent chain into the membrane adjacent to translocon proteins Sec61α and TRAM. This insertion of PEX3 into the ER is physiologically relevant because PEX3 then exits the ER via budding vesicles in an ATP-dependent process. This study identifies early steps in human peroxisomal biogenesis by demonstrating sequential stages of PMP passage through the mammalian ER.

Keywords budding vesicles, endoplasmic reticulum, human peroxisomal membrane protein PEX3, peroxisomal biogenesis, Sec61 translocon

Received 3 June 2015, revised and accepted for publication 13 November 2015, uncorrected manuscript published online 17 November 2015, published online 21 December 2015

The significance of peroxisomes in cellular metabolism is illustrated by the existence of severe inherited human diseases that result from the failure of peroxisomal biogenesis (1,2). More than 30 proteins (termed peroxins) are involved in peroxisomal assembly across species (reviewed in 3–5), but only three are key players in early peroxisomal membrane biogenesis. PEX19 is a soluble protein that acts as receptor and chaperone for newly synthesized peroxisomal membrane proteins (PMPs) in the cytosol (6). The integral PMP PEX16 mediates the endoplasmic reticulum (ER)-to-peroxisome trafficking of PMPs (7,8), but homologues are absent in most yeast species (9). The PEX3 PMP is highly conserved among species and has been proposed to be the docking factor for cytosolic PEX19•cargoPMP complexes (10,11). In yeast, PEX3 is also involved in organelle inheritance and peroxisomal autophagic degradation (pexophagy) (12,13).

The copyright line for this article was changed on 25 May after original online publication.

Peroxisomes have long been considered to be autonomous organelles that arise exclusively by growth and division of pre-existing peroxisomes (14,15). However, convincing evidence has recently shown that at least a subpopulation of PMPs in yeast (16–22), plant (23) and vertebrate cells (24–27) are targeted first to the ER prior to being transported to the peroxisomes via an ER-derived vesicle carrier (28–30). This ER-mediated biogenesis pathway also emphasized the key roles of PEX3 and PEX19 in early peroxisomal assembly, due to their newly identified functions in intra-ER sorting of PMPs, and the budding of preperoxisomal vesicles (19,22,28,29). Eventually, the combined evidence that certain PMPs are sorted either indirectly through the ER or directly to pre-existing peroxisomes evolved into the semiautonomous model of peroxisomal biogenesis (23), where both pathways are supposed to operate simultaneously (3,31–34).

As a prerequisite to understanding the early ER-mediated steps in peroxisomal biogenesis, it is essential to ascertain how peroxins are targeted to and inserted into the ER membrane. For the small group of tail-anchored PMPs, two pathways have been identified as being involved: Insertion of mammalian PEX26 is mediated by PEX19 and PEX3 (35), whereas yeast tail-anchored PMPs are most likely post-translationally inserted via the GET3 pathway (20,36). However, the majority of PMPs are polytopic or type I/II integral membrane proteins. In yeast, such PMPs appear to be inserted through the yeast Sec61p translocon (20,21) that serves as the primary ER entry point for integral membrane and secretory proteins. Depending on its exact protein composition, the yeast Sec61p complex promotes co- and post-translational translocation of proteins (37,38). Which of these pathways is taken for the translocation of yeast PMPs is unknown, because previous studies (20,21) did not reveal any mechanistic details about how the yeast Sec61p complex facilitates PMP insertion into the ER bilayer. In addition, it remains unresolved how yeast or mammalian PMPs are selected for ER insertion rather than being targeted to pre-existing peroxisomes. Making things even more complicated is the fact that the underlying molecular mechanisms may be different in species that are evolutionarily diverse. For instance, the function and topology of a critical component in early human peroxisomal biogenesis, PEX16 (39), varies between species: it is an integral membrane protein functioning as a PMP receptor in mammals (11,25), a peripheral membrane protein involved in peroxisomal fission in *Yarrowia lipolytica* (40), and most yeast species lack a PEX16 homologue (41,42). Hence, it is not always appropriate to extrapolate the knowledge gained from one organism to another evolutionarily diverse species (43), especially for complex mechanisms such as those that facilitate the ER targeting and insertion of PMPs.

With regard to their important role in human metabolism, surprisingly little is known about the passage of PMPs through the mammalian ER, including the identity of the translocon, if any, that facilitates PMP membrane insertion. In addition, it is not known whether ER-derived vesicles play a role in mammalian PMP trafficking to peroxisomes, and no suitable *in vitro* system has been established to address this issue. In this study, we identify sequential stages in the co-translational biogenesis of a human PMP, PEX3, as it enters and exits the mammalian ER. We show for the first time that the signal recognition particle (SRP) targets a peroxisomal integral membrane protein to the ER, and that PEX3 integration into the mammalian ER membrane occurs co-translationally at the Sec61-translocon in a multistep process. We also establish a mammalian cell-free membrane budding assay as an experimental platform to reveal that PMP-containing vesicles are released from the ER in an energy-dependent reaction.

Results and Discussion

Approach

Convincing evidence has been provided that certain mammalian PMPs (24,25,27,44), including human PEX3 (26), are first targeted to the ER on route to the peroxisome. In light of its important role in early peroxisomal biogenesis (45), we have focused on identifying the mechanisms involved in human PEX3 targeting to and insertion into the mammalian ER membrane. Thus, we used an *in vitro* translation system well established for studying ER targeting (46,47), the co-translational SRP/translocon-dependent targeting and integration of nascent proteins into the ER membrane (37,38,48,49), and transient nascent protein interactions during translation (50).

As soon as a cleavable signal sequence or an uncleaved signal-anchor sequence of an integral membrane protein

emerges from the ribosome, it is recognized and bound by the SRP (reviewed in 37, 38). This interaction transiently arrests protein synthesis until the SRP interacts with its ER-resident receptor to target the ribosome•nascent chain complex (RNC) to a translocon in the ER membrane. Two hydrophobic regions, HR1 and HR2 (Figure 1A), have been identified in human PEX3 (51). Since HR1 emerges first from the ribosomal exit tunnel during ribosomal synthesis (Figure 1B), its interactions were examined using environmentally sensitive probes. A photoreactive crosslinking probe (5-azido-2-nitrobenzoyl, ANB) or a fluorescent dye (7-nitrobenz-2-oxa-1,3-diazole, NBD) was positioned in the middle of HR1 by *in vitro* translation of a human PEX3 mRNA in which codon 25 was replaced by an amber stop codon (PEX3^{G25amb}, see also Figure 3A). Addition of amber suppressor aminoacyl-tRNA analogs εANB-Lys-tRNA^{amb} or εNBD-Lys-tRNA^{amb} (52–54) to the translation then allowed selective labeling of HR1 with the probe. When a truncated PEX3 mRNA transcript lacking a final stop codon was translated, all nascent chains in the resulting RNC sample had the same length and remained attached to the ribosome as peptidyl-tRNA because normal termination was prevented. By varying the length of truncated mRNA added to translations, RNCs with different nascent chain lengths provided a series of static snapshots of sequential stages in PMP membrane targeting and integration. Nascent chains are designated P(x)-PEX3(n) to represent PEX3 nascent chains with a length of n residues and a probe P at residue x. Since the ribosomal exit tunnel encloses roughly 40 residues of an emerging nascent chain, and HR1 extends until residue 36 of PEX3, a RNC with a nascent chain of approximately 80 residues is necessary to fully expose HR1 to the cytosol. Hence, initial experiments were performed with PEX3(93)-RNCs (Figure 1B), thereby ensuring sufficient spatial flexibility and distance between HR1 and the ribosome.

SRP binds the N-terminal HR1 of ribosome-bound nascent PEX3

Photoreactive ANB was introduced into HR1 by translating a truncated PEX3^{G25amb} mRNA in the presence of εANB-Lys-tRNA^{amb}; the control sample received Lys-tRNA^{amb}. The resulting ANB(25)-PEX3(93) and PEX3(93) RNCs were photolyzed, and a prominent photoadduct of approximately 65 kDa, which represents the molecular weigh of SRP54 (54 kDa) covalently linked to the PEX3 93mer (11 kDa), was formed only in the sample with ANB (Figure 1C). Photoadducts were then analyzed by immunoprecipitation using antibodies specific for SRP54, the signal sequence-binding component of SRP (55,56). Since [^{35}S]Met-labeled ANB(25)-PEX3(93) chains reacted covalently with SRP54 (Figure 1C), the photoreactive ANB in HR1 was adjacent to SRP54. On the other hand, the shorter ANB(25)-PEX3(61) RNC, which does not expose HR1 completely to the cytosol, did not form covalent photoadducts with SRP54 (Figure S1, Supporting Information). Thus, HR1 was recognized and bound by SRP as it emerged from the ribosome.

The association of SRP with PEX3-containing RNCs was also detected using a NBD fluorescent probe in HR1. NBD was chosen because its emission properties change dramatically upon moving from an aqueous to a hydrophobic environment (52), and we previously showed that NBD was a sensitive spectral sensor of SRP association with a RNC signal sequence (53). NBD was introduced at position 25 of HR1 by translating truncated PEX3^{G25amb} mRNA in the presence of εNBD-Lys-tRNA^{amb}. When canine SRP was added to purified NBD(25)-PEX3(93)-RNCs, a significant increase in NBD emission intensity was observed (Figure 1D, top). In contrast, no increase in emission intensity was detected when only buffer was added to NBD(25)-PEX3(93) RNCs (Figure S2) or when SRP was incubated with NBD(25)-PEX3(42) RNCs (Figure 1D, bottom) with HR1 still inside the ribosomal exit tunnel (Figure 1B). Moreover, SRP binding to NBD(25)-PEX3(93)-RNCs was saturable, as shown by the dependence of sample emission intensity on the concentration of SRP (Figure 1E). These data therefore provide the first direct evidence that a nascent peroxisomal integral membrane protein is recognized and bound by the SRP as soon as it emerges form the ribosomal exit tunnel.

HR1 functions as signal-anchor sequence in SRP-dependent PEX3 targeting to and integration into the ER membrane

The HR1 interaction with SRP indicates that the nonpolar HR1 acts as a signal sequence. Does HR1 also function as a transmembrane segment (TMS) to anchor PEX3 in the membrane? PEX3 HR segments were engineered into the *Escherichia coli* inner membrane protein leader peptidase (57) (Figure 2A), and the glycosylation pattern

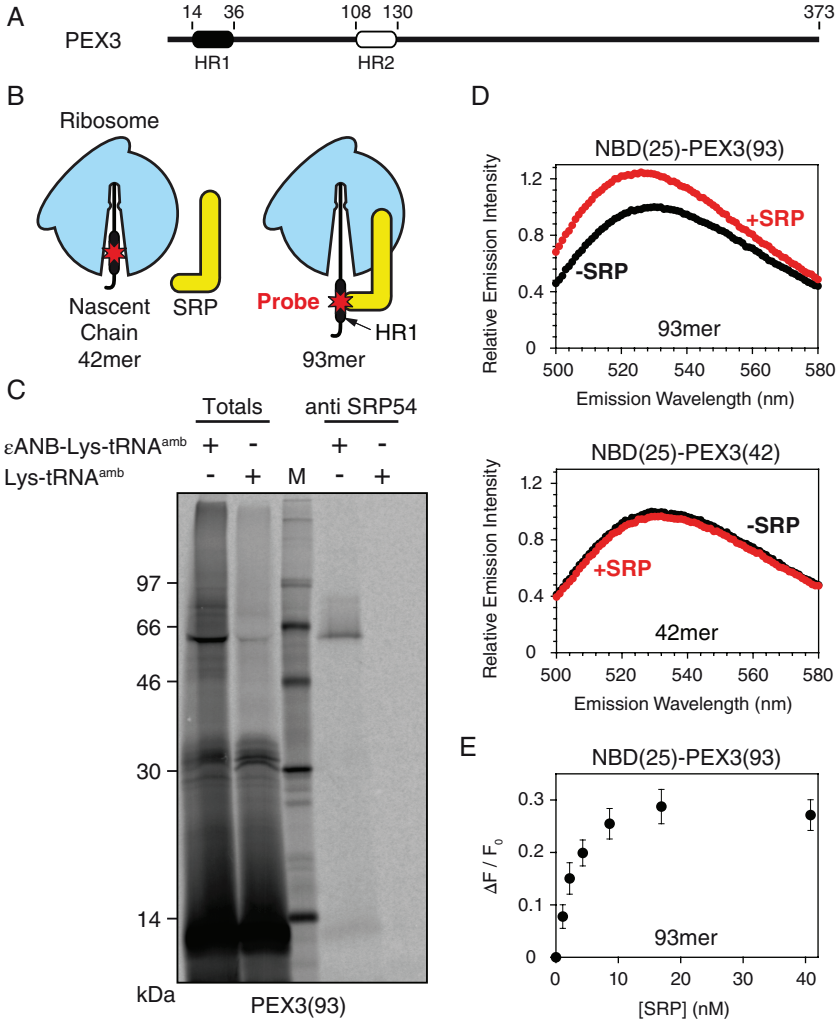

Figure 1: HR1 of PEX3 binds to SRP. A) Schematic representation of full-length PEX3. Two predicted hydrophobic α-helical regions are indicated by black (HR1) and white (HR2) boxes. B) A probe (the photoreactive crosslinker ANB or the fluorescent dye NBD) is incorporated into HR1 of ribosome-tethered nascent PEX3. The HR1 of short nascent chains (e.g. 42mer) is located within the ribosomal exit tunnel, whereas longer chains (e.g. 93mer) expose HR1 to the cytosol and hence to the SRP. C) Photocrosslinking of PEX3 to SRP. [^{35}S]Met-PEX3(93)-RNCs with or without a single ANB at residue 25 were photolyzed and then analyzed by SDS-PAGE and phosphorimaging either directly (Totals, 1/20 aliquot) or after immunoprecipitation with antibodies directed against SRP54. M: molecular weight marker. D) Fluorescence-detected SRP binding to PEX3. Emission scans ($\lambda_{ex} = 468$ nm) of purified NBD(25)-PEX3(93)- or NBD(25)-PEX3(42)-RNCs were performed in buffer A before (−SRP) and immediately after the addition of purified canine SRP (+SRP). E) Purified NBD(25)-PEX3(93)-RNCs were titrated with the indicated total concentrations of SRP. The observed change in emission intensity ($\lambda_{ex} = 468$ nm; $\lambda_{em} = 528$ nm) is ΔF, and the initial fluorescence intensity of the sample without SRP is designated F_0. The averages of at least three independent experiments are shown, with error bars indicating the SD.

revealed that isolated HR1, but not HR2, was efficiently integrated into the ER membrane (Figure 2B). Moreover, single-glycosylation of a Lep-derived chimera that contained both HRs (connected by their natural-occurring linker sequence) suggests that only one bilayer-spanning segment (HR1) exists within the HR1-HR2 fragment of PEX3 (Figure 2B). Furthermore, carbonate extraction of PEX3 and a derivative lacking HR1 (Figure 2C) showed that HR1 is necessary (Figure 2D) and sufficient (Figure S3) for stable insertion of PEX3 into the ER

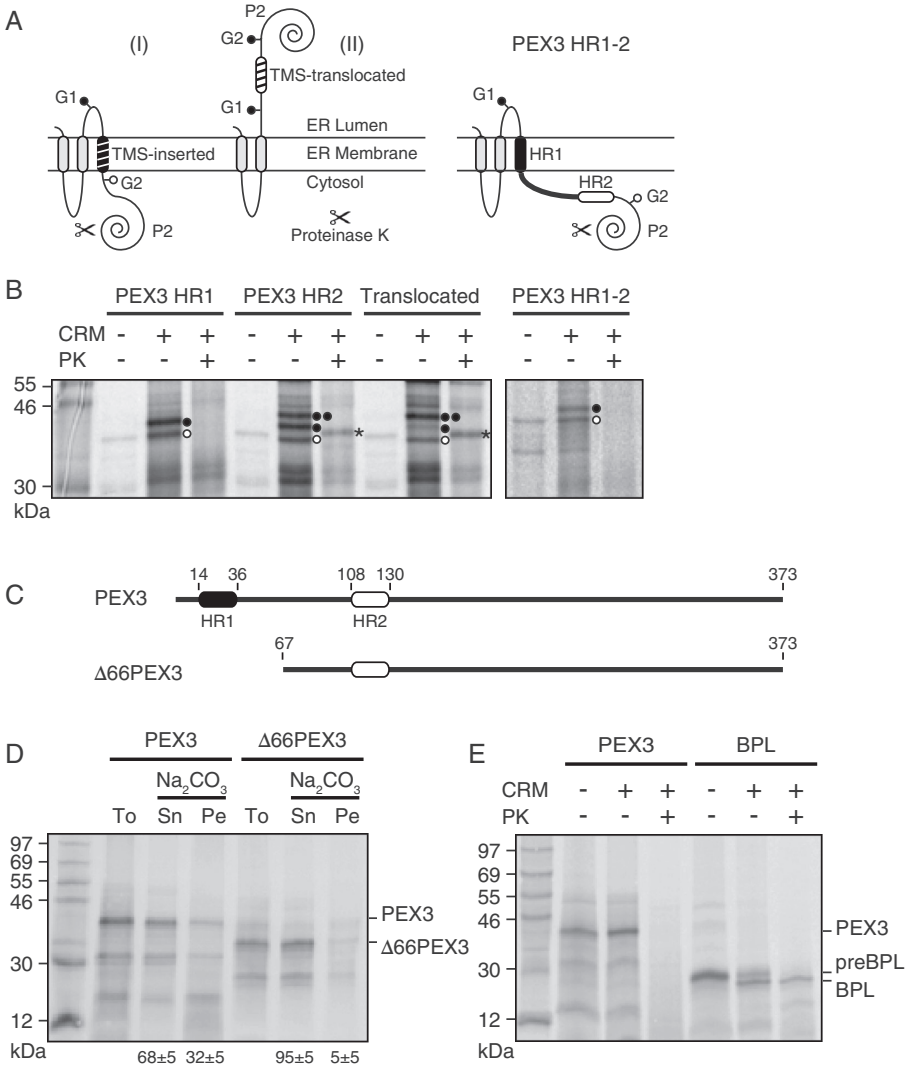

Figure 2: HR1 is responsible for ER membrane insertion of PEX3. A) Schematic representation of *E. coli* leader peptidase (Lep) constructs. A putative TMS (shaded) is engineered into the P2 domain flanked by two glycosylation acceptor sites (G1 and G2). Membrane integration of the TMS prevents enzymatic glycosylation of G2 on the lumenal side of the membrane (I), whereas both sites are glycosylated when a TMS does not insert into the membrane (II). In the latter case, ER-lumenal P2 is also protected from Proteinase K (PK) treatment. The model of a Lep construct containing both HRs of PEX3 (PEX3 HR1-2) suggests that only HR1 is inserted into the membrane. B) Insertion of PEX3 HR1 (residues 14–36), HR2 (residues 108–130), or HR1-HR2 (residues 14–130) fragments into the ER bilayer. PEX3-HR-Lep chimeras or a translocated control (construct no. 67; 58) were translated in RRL in either the presence or absence of column-washed rough microsomes (CRM). [^{35}S]Met-labeled proteins were analyzed directly or treated with PK. Unglycosylated (○), mono- (●), double-glycosylated (●●), and P2-containing protease-protected fragments (*) are indicated. C) Scheme of full-length and truncated PEX3 lacking the N-terminal 66 residues (Δ66PEX3). D) Full-length PEX3 is anchored in the ER bilayer. [^{35}S]Met-PEX3 was translated in RRL supplemented with CRM, and products were subjected to sodium carbonate extraction at pH 11.5 and separated by centrifugation. The supernatant (Sn), the membrane pellet (Pe) and an untreated aliquot (To) are shown. Numbers indicate the average amount of PEX3 or Δ66PEX3 in the supernatant and membrane pellet fractions, respectively. The averages ± SD of at least three independent experiments are shown. E) Orientation of ER-inserted PEX3. Full-length PEX3 or secreted bovine prolactin (BPL) was translated as above in either the absence or presence of CRM. Translation products were analyzed directly or treated with PK. pre, BPL with an uncleaved signal sequence.

bilayer. Finally, protease sensitivity revealed that the large C-terminal domain of ER-inserted PEX3 is exposed to the cytosol (Figure 2E), a topology previously described for peroxisomal-localized PEX3 (51,59). Since ER membrane-integrated and non-inserted PEX3 had identical molecular masses (Figure 2D,E), the N-terminal hydrophobic HR1 of PEX3 acts as a non-cleavable signal-anchor TMS that is recognized by SRP.

Following SRP•RNC docking at the ER membrane, the Sec61 translocon mediates both the transport of soluble proteins into the ER lumen and the insertion of integral membrane proteins laterally into the ER bilayer (38). The mammalian Sec61 translocon is composed of four core proteins, Sec61α,β,γ and the translocating chain-associating membrane protein (TRAM; 48). To examine SRP dependence of PEX3 targeting to the translocon, PEX3-RNCs were translated in a wheat germ extract that has such a low endogenous content of SRP that RNC targeting to canine column-washed rough microsomes (CRM) is dependent on added canine SRP (55,60). ANB(25)-PEX3(93) RNCs were prepared in the presence of CRM, and either the presence or absence of SRP. After photolysis and immunoprecipitation using antibodies specific for Sec61α, covalent photoadducts between Sec61α and PEX3 nascent chains were observed only in the presence of SRP (Figure 3B). No photoadducts were observed in the absence of the photoreactive probe (data not shown). Thus, SRP is required to target nascent PEX3 to the translocon.

PEX3 interacts with translocon proteins Sec61α and TRAM in a defined and ordered multistep sequence

To further characterize PEX3 HR1 interactions at the ER translocon, we used a high-resolution photocrosslinking approach. Parallel samples of same length ANB(23)-PEX3(79), ANB(24)-PEX3(79) and ANB(25)-PEX3(79) integration intermediates were generated and photolyzed, and the extent of photocrosslinking to translocon proteins was determined by immunoprecipitation with antibodies specific for Sec61α and TRAM. The ANBs incorporated at three sequential residues within HR1 project from three different sides of the TMS α-helix (Figure 3A). If HR1 is randomly oriented when it is proximal to Sec61α, then all three probes should react equally with Sec61α and/or TRAM. However, if an asymmetric photocrosslinking pattern is observed, then HR1 must be held in a fixed orientation adjacent to Sec61α and/or TRAM (54). Since only probes at residue 25 of PEX3 photocrosslinked to Sec61α (Figure 3C), probes at both positions 24 and 25 photocrosslinked to TRAM (Figure 3D), and probes at residue 23 photocrosslinked to neither translocon protein, the asymmetry of photocrosslinking reveals that HR1 is bound and held at a specific site within the translocon.

HR1 proximity to translocon proteins was then examined as a function of nascent chain length. Since an εANB-Lys at PEX3 residue 25 photocrosslinked to both Sec61α and TRAM, ANB(25)-PEX3 RNCs with increasing nascent chain lengths were prepared in parallel, photolyzed and analyzed by immunoprecipitation. When nascent chain length increased beyond 93 residues, HR1 was no longer adjacent to Sec61α (Figure 3E,F). TRAM-containing photoadducts were observed with nascent chain lengths of 93 and 122, 148 to a lesser extent (Figure 3F), and not at all for nascent chains 192 or more residues (Figure S4). Since HR1 was adjacent to TRAM, but not to Sec61α, at 122 residues, HR1 was retained next to TRAM longer than to Sec61α, consistent with earlier data showing a TMS passing sequentially from Sec61α to TRAM during integration at the translocon (61,62). Human PEX3 therefore inserts co-translationally into the ER membrane via a SRP-dependent and defined translocon-mediated multistep pathway.

In yeast, the only peroxin mRNA that co-localized at the ER was that of PEX3 (63), a result indirectly suggesting that the Sec61p translocon facilitates the co-translational insertion of PEX3 into the yeast ER. Other recent studies support the involvement of the yeast Sec61p translocon in PMP integration (20,21), whereas previous reports (64) came to the opposite conclusion. By taking all differences in the experimental setups into account, there is now an increasing appreciation that the yeast Sec61p translocon is required for PMP insertion into the yeast ER (reviewed in 31, 32, 65, 66). However, several key issues remain unresolved. It is not known how PMPs reach the translocon in yeast, or whether PMP insertion into the yeast ER occurs co- or post-translationally (21). Similarly, it was not known whether the Sec61 translocon was required for PMP insertion into the ER in mammals. But here we show for the first

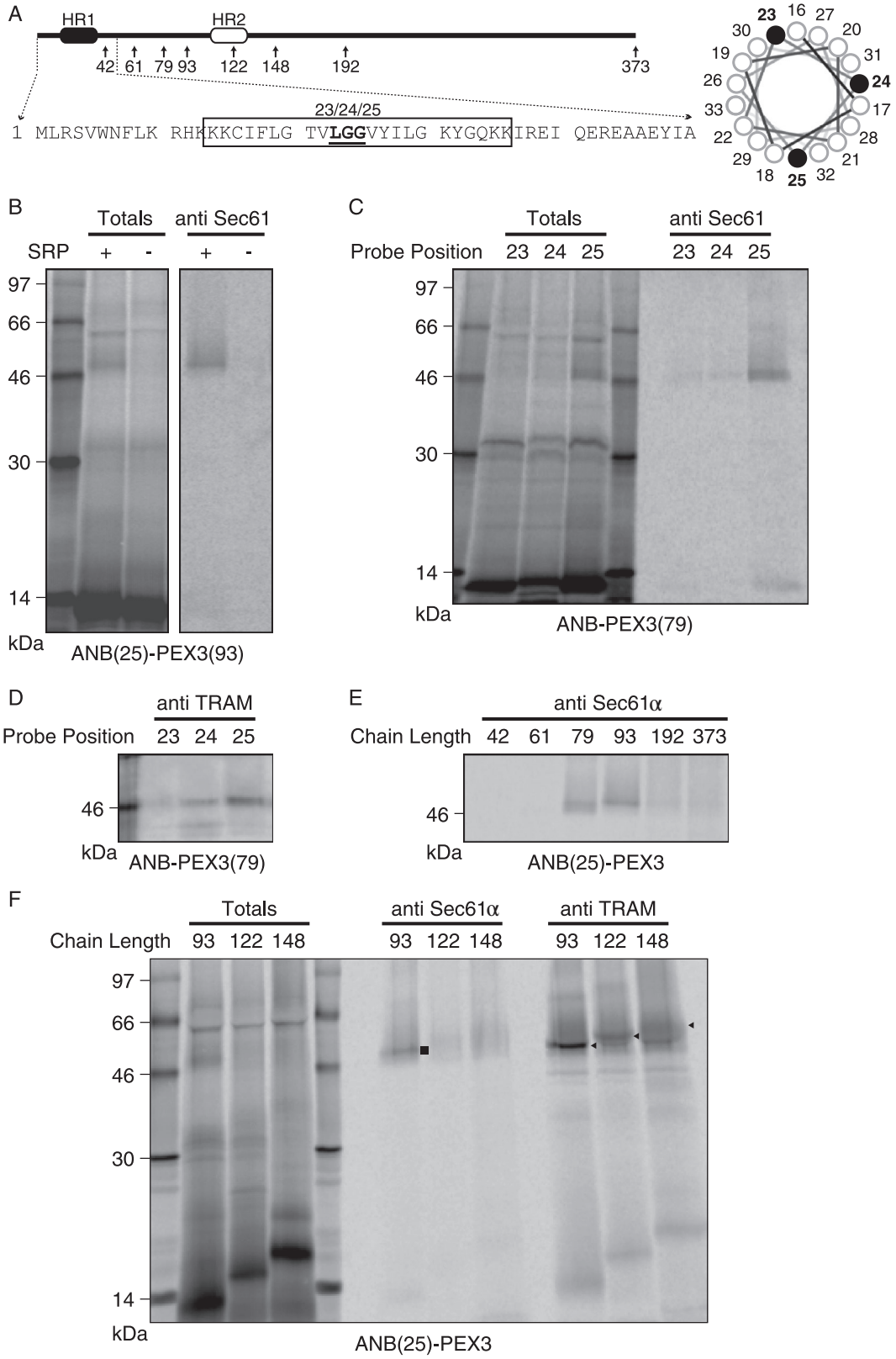

Figure 3: Legend on Next page.

time that a N-terminal TMS of a nascent PMP is recognized by SRP as it emerges form the ribosome (Figure 1), and that SRP is required to target the PMP-containing RNC to the translocon (Figure 3). These results are in line with recent data showing that the first TMS of PEX16 is necessary for its targeting to the ER(8). In addition, our data show that the nascent chain of the mammalian PMP PEX3 is co-translationally inserted into the ER bilayer adjacent to the translocon proteins Sec61α and TRAM in a multistep process (Figure 3). These results therefore establish the Sec61 translocon as ER entry point for mammalian PMPs, as well as providing mechanistic details of PMP targeting to and insertion into the mammalian ER membrane.

Does every human PEX3 insert into the ER membrane via the SRP- and translocon-mediated pathway? Given the sub-stoichiometric number of SRPs relative to ribosomes (1–2 SRPs/100 yeast ribosomes (67), and 5–8 SRPs/100 mammalian ribosomes (68)), it is certainly possible that PEX3 molecules may escape recognition by SRP and be inserted post-translationally into peroxisomes (11) or the ER (25,26). On the other hand, the co-translationally inserted PEX3 in the ER may serve as docking factor for PEX19•cargoPMP complexes (10,11) and thereby concentrate other PMPs or PMP sub-complexes (30) in a spatially defined area of the ER. The initial co-translational insertion of human PEX3 at a Sec61 translocon would therefore be a critical and essential step in seeding the mammalian ER with peroxins.

PEX3 exits the ER via budded vesicles

Is PEX3 integration into the ER membrane a precursor to PEX3 transport to the peroxisome? If so, one would predict that PEX3 is segregated into specific regions of the ER membrane for budding and transport to the peroxisome (27). A cell-free vesicle budding assay recently established in yeast (28,29) shows that PMP-containing carrier vesicles are released from the ER in a cytosol- and ATP-dependent process. To determine whether human PEX3 is packed into vesicles that bud from mammalian ER membranes, full-length PEX3 was translated *in vitro* in the presence of canine ER microsomes. Following translation, membranes were collected and washed extensively to remove any peripherally attached PEX3. These microsomes were then used as donor membranes to study the ER exit of PEX3 in the presence of rabbit reticulocyte lysate (RRL), ATP and an ATP-regenerating system. After the budding reaction, the larger and more dense donor microsomal membranes were removed by medium-speed centrifugation. PEX3 was then detected in the supernatant fraction of samples containing RRL and ATP, but not in the supernatant of samples lacking either cytosol or ATP (Figure 4A). Budded PEX3 could be collected by high-speed centrifugation, was resistant to carbonate extraction, and was solubilized in detergent (Figure 4B), thereby indicating that PEX3 was localized in a membrane of small vesicles. Since 36 ± 4% of the total integrated PEX3 was recovered in the supernatant in the presence of cytosol and ATP (Figure 4A), PEX3 was apparently selected and preferentially transferred to the small ER-derived vesicles.

Great attention has been paid to the mechanisms involved in the vesicular trafficking of PMPs from ER to peroxisomes in yeast. Recent studies revealed that new peroxisomes are formed via heterotypic fusion of at least two biochemically distinct preperoxisomal vesicle pools that arise from the ER (30). However, the detailed molecular basis for the budding of these preperoxisomal

Figure 3: Photocrosslinking of nascent PEX3 to the translocon proteins Sec61α and TRAM. A) Scheme and N-terminal sequence of PEX3. Arrows indicate nascent chains of different lengths. An amber stop codon was substituted at position L23, G24 or G25 (underlined) to position the photoreactive ANB at a single nascent chain location within HR1 (boxed). Probes project from different sides of the TMS α-helix surface as shown in the helical wheel projection (right). B) Photocrosslinking to Sec61α is SRP-dependent. [^{35}S]Met-ANB(25)-PEX3(93) nascent chains were prepared in wheat germ extract supplemented with canine CRM in either the absence or presence of canine SRP. Photoadducts were analyzed directly (Totals, 1/20 aliquot) or after immunoprecipitation with antibodies specific for Sec61α. C–F) Photocrosslinking to Sec61α and TRAM. [^{35}S]Met-labeled ANB(23)-PEX3, ANB(24)-PEX3 or ANB(25)-PEX3 integration intermediates of different length were translated in the presence of CRM and SRP. Photoadducts were analyzed either directly (Totals, 1/20 aliquot) or after immunoprecipitation with antibodies directed against Sec61α or TRAM, respectively. Photoadducts containing Sec61α (■) or TRAM (◂) are indicated in (F). Uncropped images of (D) and (E) are shown in Figure S5.

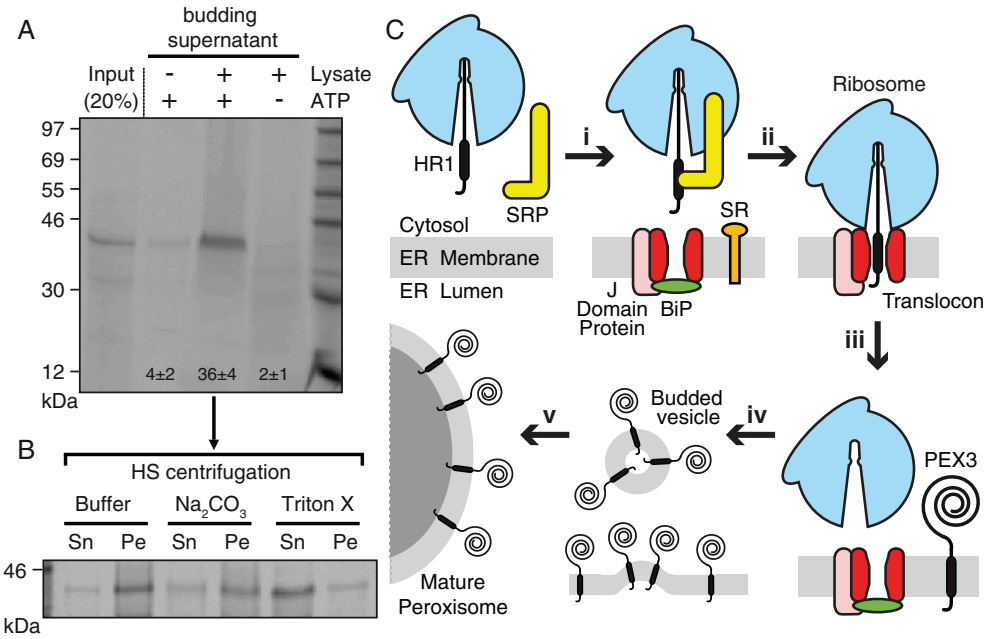

Figure 4: Cell-free vesicle budding of PEX3. A) Full-length [^{35}S]Met-PEX3 was transcribed/translated in RRL in the presence of CRM. Washed donor membranes were incubated at 30°C in the presence of either buffer A (– lysate) or RRL. Samples were either substituted with an ATP-regenerating system (+ATP) or treated with apyrase (–ATP). After the budding reaction, donor membranes were removed by sedimentation, and the supernatant fraction and a 20% aliquot (Input) of the starting microsomes were analyzed. Numbers indicate the average amount of budded PEX3 ± SD for at least three independent experiments. B) The supernatant of an ATP- and lysate-containing budding reaction was subjected to high-speed (HS) centrifugation, and the pellet was resuspended in buffer A with or without 1% (v/v) Triton X-100 or subjected to 0.1 M sodium carbonate extraction at pH 11.5. After a second centrifugation step, the protein contents of the supernatant (Sn) and pellet (Pe) fractions were analyzed. C) Model of human PEX3 passage through the ER. During ribosomal translation of PEX3, HR1 is recognized and bound by SRP (i). After SRP-dependent targeting of the RNC to the ER membrane (ii) via the SRP receptor (SR), PEX3 is co-translationally integrated into the mammalian ER at the Sec61 translocon and its associated proteins (J Domain Protein, BiP; 69) (iii). Following integration into the ER membrane, PEX3 is selectively packed into budding vesicles in an ATP- and cytosol-dependent process (iv). PEX3-containing budded vesicles then either fuse with pre-existing peroxisomes or initiate peroxisomal *de novo* synthesis (v).

structures in yeast remains unclear (70). In mammals, it was unknown whether small ER-derived vesicles play a role in the mammalian peroxisomal *de novo* biogenesis. But our data now provide the first direct evidence that human PMPs are actively and selectively extracted from mammalian ER membranes in a cytosol-dependent and ATP-consuming vesicle budding reaction. As previously reported in yeast (19,28–30), these data are consistent with small ER-derived vesicles playing a role in PEX3 trafficking to mammalian peroxisomes. By establishing a mammalian cell-free budding assay, we provide a new experimental platform that can both examine the precise distribution and binding partners of newly inserted PMPs in the ER, and identify the components in the cytosol that are involved in the budding reaction. Such information is crucial for understanding the *de novo* formation of peroxisomes from the ER in mammals.

The combined data presented here establish that nascent human PEX3 is targeted to the mammalian ER membrane by SRP, integrates co-translationally at the mammalian translocon, and then is selectively packaged and extracted from the ER membrane via an energy- and cytosol-dependent budding reaction. By experimentally characterizing the entire pathway required for PEX3 passage through the ER (Figure 4C), the transient role

of the ER in mammalian peroxisomal biogenesis has now been demonstrated from recruitment and entry to exit and discharge. On the other hand, it has been reported that certain integral PMPs, including PEX3 (11), can insert post-translationally into mature peroxisomes (6,10,35). The existence of these two distinct pathways, the co-translational insertion into the ER via the Sec61 translocon as detailed in this study, and the post-translational insertion into mature peroxisomes (6,10,11,35), is in good agreement with the currently widely accepted semiautonomous model of peroxisomal biogenesis (3,31–34). According to this working model, a dynamic peroxisomal homeostasis is ensured by both the recruitment of PMP-containing membranes from the ER via budded vesicles and the enhanced accumulation of PMP and matrix proteins in pre-existing peroxisomes, thereby facilitating fast peroxisomal propagation by growth and division. Since differences in the relative contribution of these two routes are likely to depend on the organism or its cellular conditions, a future challenging goal is to determine what fraction of PMPs, and particularly PEX3 molecules, is inserted directly into pre-existing peroxisomes instead of transiting through the ER. While the mechanisms that regulate when, where and how a PMP will follow a particular route are currently unknown, the data herein show that co-translational mammalian PEX3 targeting to and insertion into the ER membrane occurs via SRP and the Sec61 translocon, and that PEX3 exit from the mammalian ER occurs via budded vesicles in an ATP-dependent process. By establishing the mechanisms of PEX3 entry into and exit from the mammalian ER, the regulation of PEX3 trafficking can now be addressed and quantified directly.

Materials and Methods

Plasmids, mRNA, tRNA, SRP and microsomes

All PEX3 constructs originated from the plasmid pcDNA3.1/PEX3mychis that encodes the human full-length PEX3, as previously described (51). The introduction of a single amber stop codon at selected locations was done using the Quikchange protocol (Agilent Technologies). Bovine prolactin is encoded in the plasmid pSP64-BPL (71). For the membrane insertion of isolated PEX3-segments, HR1 (residues 14–36), HR2 (residues 108–130) or HR1-HR2 (residues 14–130) fragments were independently amplified and introduced into the modified *E. coli* leader peptidase (Lep) sequence from the pGEM1 plasmid (58) using the *Spe*I/*Kpn*I sites. The primary sequence of each construct was confirmed by DNA sequencing. mRNA was transcribed *in vitro* using SP6 RNA polymerase and PCR-generated DNA fragments of the desired length as before (54). Reverse primers either contained an ochre stop codon to obtain full-length PEX3 translation products (e.g. for the budding assay) or lacked a stop codon for the generation of RNCs. Primer sequences are available from the authors on request. [^{14}C]Lys-tRNA^{amb}, εANB-[^{14}C]Lys-tRNA^{amb}, εNBD-[^{14}C]Lys-tRNA^{amb}, canine CRM and purified SRP from dog pancreas in SRP buffer [50 mM triethanolamine (pH 7.5), 600 mM KOAc (pH 7.5), 6 mM $Mg(OAc)_2$, 1 mM DTT] were obtained from tRNA Probes. SRP concentration was determined using $\varepsilon_{280nm} = 1.0 \times 10^6\ M^{-1}cm^{-1}$.

Cell-free translation in RRL

In vitro translation of purified mRNA (typically 25 µL, 30°C, 40 min) was performed in the presence of RRL (Promega), [^{35}S]Met (0.4 µCi/µL), and, when indicated, 4 equivalents (eq., 72) CRM. After translation, samples were either analyzed directly by SDS-PAGE and phosphorimaging (PharosFX molecular imager, Bio-Rad), or membranes were collected by sedimentation (Beckman TLA100 rotor; 430 000 × g; 5 min; 4°C) through a 0.5 M sucrose cushion in buffer A [30 mM HEPES (pH 7.5), 120 mM KOAc, 3.2 mM $Mg(OAc)_2$]. For proteolysis experiments (Figure 2E), samples were treated with 200 µg/mL proteinase K for 30 min on ice followed by the addition of 1 mM phenylmethylsulfonyl fluoride. For carbonate extraction (73), membranes were incubated in carbonate buffer [0.1 M Na_2CO_3 (pH 11.5)] for 15 min on ice, centrifuged (Beckman TLA100 rotor; 430 000 × g; 5 min; 4°C), washed and resuspended in carbonate buffer. The supernatant and pellet fraction were neutralized with glacial acetic acid and further analyzed as above.

Lep-derived constructs were transcribed and translated in the presence of RRL, [^{35}S]Met and canine CRM as described previously (74). Samples were analyzed by SDS-PAGE, and visualized on a Fuji FLA3000 phosphorimager using ImageGauge software. The proteinase K digestions were performed after *in vitro* translation by incubation the mixture with 400 µg/mL proteinase K on ice for 40 min (Figure 2B). The reaction was stopped by adding 2 mM phenylmethylsulfonyl fluoride. The membrane fraction was then collected by centrifugation and analyzed by SDS-PAGE.

Photocrosslinking and immunoprecipitation

In vitro translations (typically 50 µL, 26°C, 40 min) of truncated mRNAs were performed in wheat germ cell-free extract (tRNA Probes) in the presence of 40 nM canine SRP, 8 eq. CRM, [^{35}S]Met (1.0 µCi/µL), 0.6 pmol/µL [^{14}C]Lys-tRNA^{amb}/εANB-[^{14}C]Lys-tRNA^{amb} as indicated, and other components as described (52). Samples were photolyzed on ice for 15 min using a 500 W mercury arc lamp (54). After photolysis, samples were collected by sedimentation (5 min for CRM or 60 min for free RNCs) through a 0.5 M sucrose cushion in buffer A as described above. Pellets were resuspended in 3% (w/v) SDS and 50 mM Tris–HCl (pH 7.5), then incubated at 55°C for 30 min. Samples were brought up to 500 µL with either buffer S [140 mM NaCl, 10 mM Tris–HCl (pH 7.5), and 2% (v/v) Triton X-100] for Sec61α-specific antibodies, or buffer T [150 mM NaCl, 1 mM EDTA, 50 mM Tris–HCl (pH 7.5), 1% (v/v) Triton X-100] for TRAM- or SRP54-specific antibodies. Samples were

precleared by rocking with protein A-Sepharose (Sigma-Aldrich; 40 µL; pre-equilibrated in buffer S or T) at 4°C for 1 h. After removal of the beads by centrifugation, the supernatants were incubated overnight at 4°C with affinity-purified rabbit antisera specific either for Sec61α or TRAM (54), or for SRP54 (BD Biosciences). Protein A-Sepharose (40 µL, pre-equilibrated with buffer S or T) was then added and incubated for 4 h at 4°C. Sepharose beads were harvested by sedimentation and washed twice with 750 µL of buffer S or T, followed by a final washing in the same buffer without detergent. Samples were then analyzed by SDS-PAGE and phosphorimaging.

Fluorescence spectroscopy

In vitro translations (500 µL total volume, 26°C, 40 min) of truncated mRNAs were performed in wheat germ cell-free extract in the presence of 0.6 pmol/µL εNBD-[^{14}C]Lys-tRNA^{amb} and other components as described (52). To correct for the significant background signal due to light scattering from the ribosomes, equivalent blank translation reactions lacking NBD were prepared in parallel with [^{14}C]Lys-tRNA^{amb}. RNCs were purified by gel filtration at 4°C using a Sepharose CL-6B column (1.5 cm inner diameter × 20 cm) and buffer A as elution buffer. A slow flow rate was used during gel filtration to ensure the removal of noncovalently bound fluorophores. The absorbance at 260 nm of each 550 µL fraction was used to identify those fractions containing RNCs that elute in the void volume, and only the leading half of the void volume peak was pooled. After gel filtration, the absorbance at 260 nm of the two parallel samples (one with and one without NBD) was equalized before initiating spectral measurements. Steady-state fluorescence measurements were made with either an SLM-8100 or a Spex Fluorolog-3 spectrofluorometer at 4°C as described previously (53). Samples (250 µL) were placed in 4 × 4 mm quartz microcells that were coated with phosphatidylcholine vesicles to minimize protein adsorption (75). The cuvette chamber was continuously flushed with N_2 to prevent condensation of water on the microcells. Emission intensity ($\lambda_{ex} = 468$ nm) was scanned at 1-nm intervals between 500 and 580 nm. Samples of purified RNCs with or without NBD in buffer A were titrated at 4°C by the sequential addition of known amounts of SRP in small volumes. After each addition, the emission intensities of the NBD and blank samples were measured after reaching equilibrium. After blank subtraction and dilution correction, the observed change in net NBD emission intensity (ΔF; $\lambda_{ex} = 468$ nm; $\lambda_{em} = 528$ nm, bandpass 4 nm) at each point in the titration was compared with the initial intensity (F_0) of the sample in the absence of SRP.

Budding assay

Purified full-length PEX3 mRNA was translated in RRL in the presence ER microsomes as described above. The translation (60 min, 30°C) was stopped by addition of puromycin (2 mM final, 20 min, 4°C) and microsomes were collected by centrifugation through a 0.5 M sucrose cushion in buffer A as above. Membranes were incubated in 2.5 M urea in buffer A for 10 min at 4°C to remove peripherally bound PEX3 molecules. Membranes were collected by medium-speed centrifugation (20 000 × ***g***, 10 min, 4°C), washed once in urea buffer, and finally washed in buffer A. Such PEX3 containing donor membranes were resuspended in buffer A, and incubated with either RRL (the lysate was diluted to 60% of its original concentration in the budding reaction) or an equivalent amount of buffer A. Budding reactions also contained 2 mM puromycin and either an energy generating system (final concentrations: 16 mM phosphocreatine, 2 mM ATP, 2 mM GTP, 0.016 U/µL phosphocreatine kinase) or 1 U/µL apyrase. After incubation of the budding reaction for 60 min at 30°C, donor membranes were removed by medium-speed centrifugation, and the supernatant was analyzed by SDS-PAGE and phosphorimaging. In certain cases, the supernatant of a budding reaction was further subjected to high-speed centrifugation (Beckman TLA100 rotor; 55 000 rpm; 30 min; 4°C), and the pellet was resuspended in either carbonate buffer or 0.25 M sucrose in buffer A in the presence or absence of 1% (v/v) Triton X-100. After a second high-speed centrifugation, the protein content of the supernatant and pellet fractions was analyzed as above.

Acknowledgments

We are grateful to Y. Miao and Y. Shao for technical assistance. This work was supported by NIH grant GM26494 (A. E. J.), by the Robert A. Welch Foundation (A. E. J., Chair grant BE-0017), and by BFU2012-39482 from the Spanish Ministerio de Economia y Competitividad and PROMETEOII/2014/061 from Generalitat Valenciana (I. M.). M. B.-P. was recipient of FPU predoctoral fellowship. P. U. M., M. B. P., and I. M. declare that they have no competing financial interests. A. E. J. is a founder of tRNA Probes, LLC.

Supporting Information

Additional Supporting Information may be found in the online version of this article:

Figure S1: Photocrosslinking of PEX3(61)- and PEX3(93)-RNCs to SRP. [^{35}S]Met-ANB(25)-PEX3-RNCs were photolyzed and then analyzed by SDS-PAGE and phosphorimaging either directly (Totals, 1/20 aliquot) or after immunoprecipitation with antibodies directed against SRP54. Photoadducts containing SRP54 (♦) are indicated.

Figure S2: SRP storage buffer does not alter the emission intensity of fluorescence-labeled PEX3. Truncated PEX3^{G25amb} mRNA was translated in wheat germ extract in the presence of εNBD-Lys-tRNA^{amb}. Emission scans ($\lambda_{ex} = 468$ nm) of purified NBD(25)-PEX3(93)-RNCs were performed in buffer A before (−SRP buffer) and immediately after the addition of SRP storage buffer (+SRP buffer, equal volume as in Figure 1D).

Figure S3: HR1 of PEX3 is stably anchored in the ER bilayer. A) Schematic representation of full-length PEX3 and a C-terminally truncated PEX3 variant of 79 residues length (PEX[79]). Two predicted hydrophobic α-helical regions (HR) are indicated by black (HR1) and white (HR2) boxes. B) PEX[79] was translated in rabbit reticulocyte lysate in the presence of CRMs. [^{35}S]Met-labeled translation products were subjected to sodium carbonate extraction at pH 11.5. After centrifugation (100 000 × ***g***; 20 min), the supernatant (Sn) and the membrane pellet (Pe) were analyzed by SDS-PAGE and visualized by phosphorimaging.

Figure S4: Photocrosslinking of PEX3 to TRAM depends on nascent chain length. [^{35}S]Met-labeled integration intermediates containing ANB(25)-PEX3 nascent chains were prepared in parallel in wheat germ extract (supplemented with canine ER microsomal membranes and 40 nM canine SRP) with lengths of 42, 61, 79, 93, 192 and 373 (full-length) residues. After photolysis, photoadducts were immunoprecipitated with antibodies directed against TRAM and analyzed by SDS-PAGE and phosphorimaging.

Figure S5: Uncropped phosphorimager scans of Figure 3D,E.

References

1. Lazarow PB, Moser HW. Disorders of peroxisome biogenesis. In: Scriver CR, Beaudet AL, Sly WS, Valle D, editors. The Metabolic and Molecular Bases of Inherited Disease. New York: McGraw-Hill; 1995, pp. 2287–2324.
2. Fujiki Y, Yagita Y, Matsuzaki T. Peroxisome biogenesis disorders: molecular basis for impaired peroxisomal membrane assembly: in metabolic functions and biogenesis of peroxisomes in health and disease. Biochim Biophys Acta 2012;1822:1337–1342.
3. Fujiki Y, Okumoto K, Mukai S, Honsho M, Tamura S. Peroxisome biogenesis in mammalian cells. Front Physiol 2014;5:307.
4. Hettema EH, Erdmann R, van der Klei I, Veenhuis M. Evolving models for peroxisome biogenesis. Curr Opin Cell Biol 2014;29:25–30.
5. Smith JJ, Aitchison JD. Peroxisomes take shape. Nat Rev Mol Cell Biol 2013;14:803–817.
6. Jones JM, Morrell JC, Gould SJ. PEX19 is a predominantly cytosolic chaperone and import receptor for class 1 peroxisomal membrane proteins. J Cell Biol 2004;164:57–67.
7. Aranovich A, Hua R, Rutenberg AD, Kim PK. PEX16 contributes to peroxisome maintenance by constantly trafficking PEX3 via the ER. J Cell Sci 2014;127:3675–3686.
8. Hua R, Gidda SK, Aranovich A, Mullen RT, Kim PK. Multiple domains in PEX16 mediate its trafficking and recruitment of peroxisomal proteins to the ER. Traffic 2015;16:832–852.
9. Fujiki Y, Matsuzono Y, Matsuzaki T, Fransen M. Import of peroxisomal membrane proteins: the interplay of Pex3p- and Pex19p-mediated interactions. Biochim Biophys Acta 2006;1763:1639–1646.
10. Fang Y, Morrell JC, Jones JM, Gould SJ. PEX3 functions as a PEX19 docking factor in the import of class I peroxisomal membrane proteins. J Cell Biol 2004;164:863–875.
11. Matsuzaki T, Fujiki Y. The peroxisomal membrane protein import receptor Pex3p is directly transported to peroxisomes by a novel Pex19p- and Pex16p-dependent pathway. J Cell Biol 2008;183:1275–1286.
12. Knoblach B, Sun X, Coquelle N, Fagarasanu A, Poirier RL, Rachubinski RA. An ER-peroxisome tether exerts peroxisome population control in yeast. EMBO J 2013;32:2439–2453.
13. Motley AM, Nuttall JM, Hettema EH. Pex3-anchored Atg36 tags peroxisomes for degradation in *Saccharomyces cerevisiae*. EMBO J 2012;31:2852–2868.
14. Fujiki Y, Rachubinski RA, Lazarow PB. Synthesis of a major integral membrane polypeptide of rat liver peroxisomes on free polysomes. Proc Natl Acad Sci USA 1984;81:7127–7131.
15. Lazarow PB, Fujiki Y. Biogenesis of peroxisomes. Annu Rev Cell Biol 1985;1:489–530.
16. Baerends RJ, Rasmussen SW, Hilbrands RE, van der Heide M, Faber KN, Reuvekamp PT, Kiel JA, Cregg JM, van der Klei IJ, Veenhuis M. The Hansenula polymorpha PER9 gene encodes a peroxisomal membrane protein essential for peroxisome assembly and integrity. J Biol Chem 1996;271:8887–8894.
17. Titorenko VI, Ogrydziak DM, Rachubinski RA. Four distinct secretory pathways serve protein secretion, cell surface growth, and peroxisome biogenesis in the yeast *Yarrowia lipolytica*. Mol Cell Biol 1997;17:5210–5226.
18. Elgersma Y, Kwast L, van den Berg M, Snyder WB, Distel B, Subramani S, Tabak HF. Overexpression of Pex15p, a phosphorylated peroxisomal integral membrane protein required for peroxisome assembly in *S. cerevisiae*, causes proliferation of the endoplasmic reticulum membrane. EMBO J 1997;16:7326–7341.
19. Hoepfner D, Schildknegt D, Braakman I, Philippsen P, Tabak HF. Contribution of the endoplasmic reticulum to peroxisome formation. Cell 2005;122:85–95.
20. van der Zand A, Braakman I, Tabak HF. Peroxisomal membrane proteins insert into the endoplasmic reticulum. Mol Biol Cell 2010;21:2057–2065.
21. Thoms S, Harms I, Kalies KU, Gartner J. Peroxisome formation requires the endoplasmic reticulum channel protein Sec61. Traffic 2012;13:599–609.
22. Fakieh MH, Drake PJ, Lacey J, Munck JM, Motley AM, Hettema EH. Intra-ER sorting of the peroxisomal membrane protein Pex3 relies on its luminal domain. Biol Open 2013;2:829–837.
23. Mullen RT, Lisenbee CS, Miernyk JA, Trelease RN. Peroxisomal membrane ascorbate peroxidase is sorted to a membranous network that resembles a subdomain of the endoplasmic reticulum. Plant Cell 1999;11:2167–2185.
24. Geuze HJ, Murk JL, Stroobants AK, Griffith JM, Kleijmeer MJ, Koster AJ, Verkleij AJ, Distel B, Tabak HF. Involvement of the endoplasmic reticulum in peroxisome formation. Mol Biol Cell 2003;14:2900–2907.
25. Kim PK, Mullen RT, Schumann U, Lippincott-Schwartz J. The origin and maintenance of mammalian peroxisomes involves a de novo PEX16-dependent pathway from the ER. J Cell Biol 2006;173:521–532.
26. Toro AA, Araya CA, Cordova GJ, Arredondo CA, Cardenas HG, Moreno RE, Venegas A, Koenig CS, Cancino J, Gonzalez A, Santos MJ. Pex3p-dependent peroxisomal biogenesis initiates in the endoplasmic reticulum of human fibroblasts. J Cell Biochem 2009;107:1083–1096.
27. Yonekawa S, Furuno A, Baba T, Fujiki Y, Ogasawara Y, Yamamoto A, Tagaya M, Tani K. Sec16B is involved in the endoplasmic reticulum export of the peroxisomal membrane biogenesis factor peroxin 16 (Pex16) in mammalian cells. Proc Natl Acad Sci USA 2011;108:12746–12751.

28. Lam SK, Yoda N, Schekman R. A vesicle carrier that mediates peroxisome protein traffic from the endoplasmic reticulum. Proc Natl Acad Sci USA 2010;107:21523–21528.
29. Agrawal G, Joshi S, Subramani S. Cell-free sorting of peroxisomal membrane proteins from the endoplasmic reticulum. Proc Natl Acad Sci USA 2011;108:9113–9118.
30. van der Zand A, Gent J, Braakman I, Tabak HF. Biochemically distinct vesicles from the endoplasmic reticulum fuse to form peroxisomes. Cell 2012;149:397–409.
31. Dimitrov L, Lam SK, Schekman R. The role of the endoplasmic reticulum in peroxisome biogenesis. Cold Spring Harb Perspect Biol 2013;5:a013243.
32. Theodoulou FL, Bernhardt K, Linka N, Baker A. Peroxisome membrane proteins: multiple trafficking routes and multiple functions? Biochem J 2013;451:345–352.
33. Veenhuis M, van der Klei IJ. A critical reflection on the principles of peroxisome formation in yeast. Front Physiol 2014;5:110.
34. Kim PK, Hettema EH. Multiple pathways for protein transport to peroxisomes. J Mol Biol 2015;427:1176–1190.
35. Yagita Y, Hiromasa T, Fujiki Y. Tail-anchored PEX26 targets peroxisomes via a PEX19-dependent and TRC40-independent class I pathway. J Cell Biol 2013;200:651–666.
36. Schuldiner M, Metz J, Schmid V, Denic V, Rakwalska M, Schmitt HD, Schwappach B, Weissman JS. The GET complex mediates insertion of tail-anchored proteins into the ER membrane. Cell 2008;134:634–645.
37. Rapoport TA. Protein translocation across the eukaryotic endoplasmic reticulum and bacterial plasma membranes. Nature 2007;450:663–669.
38. Shao S, Hegde RS. Membrane protein insertion at the endoplasmic reticulum. Annu Rev Cell Dev Biol 2011;27:25–56.
39. Honsho M, Tamura S, Shimozawa N, Suzuki Y, Kondo N, Fujiki Y. Mutation in PEX16 is causal in the peroxisome-deficient Zellweger syndrome of complementation group D. Am J Hum Genet 1998;63:1622–1630.
40. Guo T, Gregg C, Boukh-Viner T, Kyryakov P, Goldberg A, Bourque S, Banu F, Haile S, Milijevic S, San KH, Solomon J, Wong V, Titorenko VI. A signal from inside the peroxisome initiates its division by promoting the remodeling of the peroxisomal membrane. J Cell Biol 2007;177:289–303.
41. Eitzen GA, Szilard RK, Rachubinski RA. Enlarged peroxisomes are present in oleic acid-grown *Yarrowia lipolytica* overexpressing the PEX16 gene encoding an intraperoxisomal peripheral membrane peroxin. J Cell Biol 1997;137:1265–1278.
42. Kiel JA, Veenhuis M, van der Klei IJ. PEX genes in fungal genomes: common, rare or redundant. Traffic 2006;7:1291–1303.
43. Kim PK, Mullen RT. PEX16: a multifaceted regulator of peroxisome biogenesis. Front Physiol 2013;4:241.
44. Novikoff PM, Novikoff AB. Peroxisomes in absorptive cells of mammalian small intestine. J Cell Biol 1972;53:532–560.
45. Muntau AC, Mayerhofer PU, Paton BC, Kammerer S, Roscher AA. Defective peroxisome membrane synthesis due to mutations in human PEX3 causes Zellweger syndrome, complementation group G. Am J Hum Genet 2000;67:967–975.
46. Stefanovic S, Hegde RS. Identification of a targeting factor for posttranslational membrane protein insertion into the ER. Cell 2007;128:1147–1159.
47. Shao S, Hegde RS. A calmodulin-dependent translocation pathway for small secretory proteins. Cell 2011;147:1576–1588.
48. Johnson AE, van Waes MA. The translocon: a dynamic gateway at the ER membrane. Annu Rev Cell Dev Biol 1999;15:799–842.
49. Alder NN, Johnson AE. Cotranslational membrane protein biogenesis at the endoplasmic reticulum. J Biol Chem 2004;279:22787–22790.
50. Karamyshev AL, Patrick AE, Karamysheva ZN, Griesemer DS, Hudson H, Tjon-Kon-Sang S, Nilsson I, Otto H, Liu Q, Rospert S, von Heijne G, Johnson AE, Thomas PJ. Inefficient SRP interaction with a nascent chain triggers a mRNA quality control pathway. Cell 2014;156:146–157.
51. Kammerer S, Holzinger A, Welsch U, Roscher AA. Cloning and characterization of the gene encoding the human peroxisomal assembly protein Pex3p. FEBS Lett 1998;429:53–60.
52. Crowley KS, Reinhart GD, Johnson AE. The signal sequence moves through a ribosomal tunnel into a noncytoplasmic aqueous environment at the ER membrane early in translocation. Cell 1993;73:1101–1115.
53. Flanagan JJ, Chen JC, Miao Y, Shao Y, Lin J, Bock PE, Johnson AE. Signal recognition particle binds to ribosome-bound signal sequences with fluorescence-detected subnanomolar affinity that does not diminish as the nascent chain lengthens. J Biol Chem 2003;278:18628–18637.
54. McCormick PJ, Miao Y, Shao Y, Lin J, Johnson AE. Cotranslational protein integration into the ER membrane is mediated by the binding of nascent chains to translocon proteins. Mol Cell 2003;12:329–341.
55. Krieg UC, Walter P, Johnson AE. Photocrosslinking of the signal sequence of nascent preprolactin to the 54-kilodalton polypeptide of the signal recognition particle. Proc Natl Acad Sci USA 1986;83:8604–8608.
56. Kurzchalia TV, Wiedmann M, Girshovich AS, Bochkareva ES, Bielka H, Rapoport TA. The signal sequence of nascent preprolactin interacts with the 54 K polypeptide of the signal recognition particle. Nature 1986;320:634–636.
57. Hessa T, Kim H, Bihlmaier K, Lundin C, Boekel J, Andersson H, Nilsson I, White SH, von Heijne G. Recognition of transmembrane helices by the endoplasmic reticulum translocon. Nature 2005;433:377–381.
58. Martinez-Gil L, Johnson AE, Mingarro I. Membrane insertion and biogenesis of the Turnip crinkle virus p9 movement protein. J Virol 2010;84:5520–5527.
59. Soukupova M, Sprenger C, Gorgas K, Kunau WH, Dodt G. Identification and characterization of the human peroxin PEX3. Eur J Cell Biol 1999;78:357–374.
60. Tamborero S, Vilar M, Martinez-Gil L, Johnson AE, Mingarro I. Membrane insertion and topology of the translocating chain-associating membrane protein (TRAM). J Mol Biol 2011;406:571–582.

61. Do H, Falcone D, Lin J, Andrews DW, Johnson AE. The cotranslational integration of membrane proteins into the phospholipid bilayer is a multistep process. Cell 1996;85:369–378.
62. Sauri A, McCormick PJ, Johnson AE, Mingarro I. Sec61alpha and TRAM are sequentially adjacent to a nascent viral membrane protein during its ER integration. J Mol Biol 2007;366:366–374.
63. Zipor G, Haim-Vilmovsky L, Gelin-Licht R, Gadir N, Brocard C, Gerst JE. Localization of mRNAs coding for peroxisomal proteins in the yeast, *Saccharomyces cerevisiae*. Proc Natl Acad Sci USA 2009;106:19848–19853.
64. South ST, Baumgart E, Gould SJ. Inactivation of the endoplasmic reticulum protein translocation factor, Sec61p, or its homolog, Ssh1p, does not affect peroxisome biogenesis. Proc Natl Acad Sci USA 2001;98:12027–12031.
65. Agrawal G, Subramani S. Emerging role of the endoplasmic reticulum in peroxisome biogenesis. Front Physiol 2013;4:286.
66. Tabak HF, Braakman I, van der Zand A. Peroxisome formation and maintenance are dependent on the endoplasmic reticulum. Annu Rev Biochem 2013;82:723–744.
67. Raue U, Oellerer S, Rospert S. Association of protein biogenesis factors at the yeast ribosomal tunnel exit is affected by the translational status and nascent polypeptide sequence. J Biol Chem 2007;282:7809–7816.
68. Bovia F, Fornallaz M, Leffers H, Strub K. The SRP9/14 subunit of the signal recognition particle (SRP) is present in more than 20-fold excess over SRP in primate cells and exists primarily free but also in complex with small cytoplasmic Alu RNAs. Mol Biol Cell 1995;6:471–484.
69. Lin PJ, Jongsma CG, Liao S, Johnson AE. Transmembrane segments of nascent polytopic membrane proteins control cytosol/ER targeting during membrane integration. J Cell Biol 2011;195:41–54.
70. Knoops K, Manivannan S, Cepinska MN, Krikken AM, Kram AM, Veenhuis M, van der Klei IJ. Preperoxisomal vesicles can form in the absence of Pex3. J Cell Biol 2014;204:659–668.
71. Skach WR, Lingappa VR. Amino-terminal assembly of human P-glycoprotein at the endoplasmic reticulum is directed by cooperative actions of two internal sequences. J Biol Chem 1993;268:23552–23561.
72. Walter P, Blobel G. Preparation of microsomal membranes for cotranslational protein translocation. Methods Enzymol 1983;96:84–93.
73. Fujiki Y, Hubbard AL, Fowler S, Lazarow PB. Isolation of intracellular membranes by means of sodium carbonate treatment: application to endoplasmic reticulum. J Cell Biol 1982;93:97–102.
74. Martinez-Gil L, Perez-Gil J, Mingarro I. The surfactant peptide KL4 sequence is inserted with a transmembrane orientation into the endoplasmic reticulum membrane. Biophys J 2008;95:L36–L38.
75. Ye J, Esmon NL, Esmon CT, Johnson AE. The active site of thrombin is altered upon binding to thrombomodulin. Two distinct structural changes are detected by fluorescence, but only one correlates with protein C activation. J Biol Chem 1991;266:23016–23021.